Ctr9, a key subunit of PAFc, affects global estrogen signaling and drives ERα-positive breast tumorigenesis

Hao Zeng and Wei Xu

McArdle Laboratory for Cancer Research, Graduate Program in Cellular and Molecular Biology, University of Wisconsin-Madison, Madison, Wisconsin 53706, USA

The human RNA polymerase II (RNAPII)-associated factor complex (hPAFc) and its individual subunits have been implicated in human diseases, including cancer. However, its involvement in breast cancer awaits investigation. Using data mining and human breast cancer tissue microarrays, we found that Ctr9, the key scaffold subunit in hPAFc, is highly expressed in estrogen receptor α-positive ($ERα^+$) luminal breast cancer, and the high expression of Ctr9 correlates with poor prognosis. Knockdown of Ctr9 in $ERα^+$ breast cancer cells almost completely erased estrogen-regulated transcriptional response. At the molecular level, Ctr9 enhances ERα protein stability, promotes recruitment of ERα and RNAPII, and stimulates transcription elongation and transcription-coupled histone modifications. Knockdown of Ctr9, but not other hPAFc subunits, alters the morphology, proliferative capacity, and tamoxifen sensitivity of $ERα^+$ breast cancer cells. Together, our study reveals that Ctr9, a key subunit of hPAFc, is a central regulator of estrogen signaling that drives $ERα^+$ breast tumorigenesis, rendering it a potential target for the treatment of $ERα^+$ breast cancer.

[*Keywords*: PAFc; breast cancer; transcription; estrogen signaling]

Supplemental material is available for this article.

Received July 14, 2015; revised version accepted September 23, 2015.

The initiation and progression of breast cancer are controlled by complex transcriptional networks in concert with extensive chromatin modifications. In approximately two-thirds of breast cancer, proproliferative pathways that drive cancer growth are activated by estrogen receptor α (ERα)-dependent transcription (Deroo and Korach 2006). Estrogen-stimulated ERα recruits coactivators, which often carry histone modification activities, to coordinate with basal transcription machineries to achieve productive cycles of transcription (Kininis et al. 2009). Coactivator-associated arginine methyltransferase 1 (CARM1) is a potent coactivator of ERα, which specifically deposits the active histone mark H3R17me2a (Chen et al. 1999; Al-Dhaheri et al. 2011) near the promoter of target genes. We previously showed that the human RNA polymerase II (RNAPII)-associated factor complex (hPAFc) interacts directly with H3R17me2a and that this association is required for productive transcriptional initiation and elongation of the *pS2* gene in MCF7 breast cancer cells (Wu and Xu 2012).

PAFc was originally identified as a protein complex associated with RNAPII in *Saccharomyces cerevisiae*. Yeast PAFc is comprised of five subunits, including Paf1, Ctr9, Cdc73 (also known as parafibromin), Leo1, and Rtf1 (Jaehning 2010). PAFc plays a regulatory role during transcriptional initiation, elongation, and termination (Jaehning 2010; Kim et al. 2010; Crisucci and Arndt 2011). PAFc has been well characterized for its role in controlling transcription-coupled histone modifications such as histone H2B monoubiquitination (H2Bub1), H3K4 trimethylation (H3K4me3), and H3K36me3 via interacting with the respective histone-modifying enzymes (Tomson and Arndt 2013). PAFc is evolutionarily conserved from yeast to *Drosophila* and humans; however, the hPAFc differs from yeast PAFc in one subunit: Ski8 (also known as WDR61) in humans and Rtf1 in yeast. As a multisubunit complex, the protein stability of each subunit is closely interrelated and regulated by the complex stoichiometry, as deficiency in one subunit can destabilize one or more of the other subunits in both yeast PAFc and hPAFc (Mueller et al. 2004; Lin et al. 2008; Wu and Xu 2012). Moreover, structural and biochemical evidence shows that Paf1 and Leo1 form a heterodimer and that Ctr9 acts as a key scaffold protein during hPAFc assembly (Chu et al. 2013).

Corresponding author: wxu@oncology.wisc.edu
Article is online at http://www.genesdev.org/cgi/doi/10.1101/gad.268722.115.

Mutation, amplification, or deregulation of hPAFc subunits has been associated with human diseases, including cancer (Chaudhary et al. 2007); thus, subunits of hPAFc could act as tumor suppressors or oncogenes in a context-dependent manner. For example, *PAF1* is amplified in pancreatic cancer, leading to the overexpression of Paf1 protein in poorly differentiated pancreatic cancer cells (Moniaux et al. 2006). The overexpressed Paf1 regulates self-renewal and drug resistance of pancreatic and ovarian cancer stem cells (Vaz et al. 2014). In contrast, a deletion including *CTR9* was identified in some pancreatic cancer cell lines (Bashyam et al. 2005), and germline mutations in *CTR9* predispose to Wilms tumor (Hanks et al. 2014). This suggests that *CTR9* may act as a tumor suppressor in some circumstances. *Leo1* at 15q21 is amplified in colorectal cancer and malignant fibrous histiocytoma of the bone (Camps et al. 2006; Tarkkanen et al. 2006). Cdc73 is a tumor suppressor protein encoded by *HRPT2* that is mutated in the germline of hyperparathyroidism–jaw tumor syndrome patients (Carpten et al. 2002; Rozenblatt-Rosen et al. 2005). Interestingly, *HRPT2* is amplified in liver carcinoma and breast cancer (Chaudhary et al. 2007). Despite the diverse genetic alterations and functional spectrum of hPAFc subunits in disease states, specific roles for hPAFc or its subunits in breast cancer progression have not yet been identified.

In this study, the involvement of Ctr9 in ERα$^+$ breast cancer progression and global ERα transcriptional regulation is examined. Ctr9 is highly expressed in ERα$^+$ luminal breast cancer, and high Ctr9 expression strongly correlates with poor overall and recurrence-free survival of ERα$^+$ breast cancer patients. Not only is Ctr9 essential for the growth of ERα$^+$ breast cancer cells, it also enhances tamoxifen resistance in cell line models. Moreover, Ctr9 appears to be essential for the global ERα transcriptional response through its ability to stabilize ERα protein, recruit RNAPII, and stimulate histone modifications such as H2Bub1, H3K27 acetylation (H3K27ac), and H3K36me3. Taken together, our studies suggest that Ctr9 plays essential roles in regulating estrogen signaling and driving ERα$^+$ breast tumorigenesis.

Results

High expression of Ctr9 in ERα$^+$ luminal breast cancer and its correlation with poor prognosis

Human breast cancers are classified into five distinct subtypes based on gene expression profile: basal-like, ERBB2$^+$, luminal A, luminal B, and normal-like (Perou et al. 2000). To explore whether hPAFc expression varies by breast cancer subtype, we examined the mRNA levels of hPAFc subunits in 51 breast cancer cell lines using published microarray data sets (Neve et al. 2006). The results showed that *CTR9* and *PAF1* are expressed at a slightly higher level in luminal subtypes (Fig. 1A). A similar observation was made using the published GSE1456 microarray data set from 150 primary breast tumors (Fig. 1B; Pawitan et al. 2005). Further large-scale gene expression analyses of the hPAFc subunits were performed on >1000 primary breast cancers using the Breast Cancer Gene Expression Miner 3.0 (bc-GenExMiner 3.0) online tool (Jézéquel et al. 2013). Similar to the *ESR1* gene encoding the ERα protein, which is the major molecular determinant of luminal breast cancer, *CTR9* mRNA expression is highly enriched in the luminal subtypes (Supplemental Fig. S1). Moreover, we examined the hPAFc subunit protein levels in human breast cancer cell lines (Fig. 1C) and tissue samples from patient-derived xenografts (Fig. 1D). The results revealed that Ctr9 and ERα proteins were more abundant in the luminal breast cancer subtype. Together, these data suggest that the Ctr9 subunit is highly expressed in ERα$^+$ luminal breast cancer.

To determine whether high expression of Ctr9 correlates with clinical outcome in breast cancer patients, human breast cancer tissue microarrays (TMAs) containing 372 breast tumor specimens were probed with an antibody to Ctr9, optimized as shown in Supplemental Figure S2A, and the intensity of immunostaining was determined based on optical density (Fig. 1E; Supplemental Fig. S2B). The TMA data showed higher average Ctr9 expression in ERα$^+$ breast tumors ($n = 280$) than in ERα$^-$ tumors ($n = 80$) (Fig. 1F). Moreover, we stratified ERα$^+$ patients into two groups, low Ctr9 and high Ctr9, based on the median Ctr9 staining intensity. The Kaplan-Meier plot for patients with ERα$^+$ breast cancer shows that patients with higher Ctr9 expression had shorter overall survival time (Fig. 1G) as well as shorter recurrence-free survival time (Fig. 1H). These data suggest that Ctr9 could play a direct role in promoting ERα$^+$ breast tumorigenesis.

Ctr9 is required for the growth of ERα$^+$ but not ERα$^-$ breast cancer cells

To assess the functional roles of Ctr9 in ERα$^+$ breast cancer, Ctr9 expression was knocked down in MCF7 breast cancer cells using a previously established cell line model in which Ctr9 expression is turned down in the presence of doxycycline (Dox) (i.e., MCF7-tet-on–shCtr9) (Wu and Xu 2012). As shown in Figure 2, A and B, Dox treatment led to partial loss of Ctr9 after 3 d and almost complete loss after 5 or 9 d. Interestingly, the Ctr9 knockdown cells adopted an elongated and enlarged shape after 5 or 9 d of treatment with Dox (Fig. 2C), while Dox had no effect on Ctr9 expression or morphology in parental control cells (Supplemental Fig. S3A,C). The morphological change was also observed when cells were grown in estrogen-deprived medium (Supplemental Fig. S3D). Consistent with the change in cell morphology, phalloidin staining showed that the structure of the F-actin cytoskeleton was reorganized after Ctr9 knockdown (Fig. 2D). Furthermore, after Ctr9 knockdown, the fraction of G0/G1 cells detected by flow cytometry increased whether cells were grown in complete medium (Fig. 2E) or estrogen-deprived medium followed by estrogen (17 β-estradiol [E2]) treatment (Supplemental Fig. S3F). In addition, senescence-associated β-galactosidase staining depicted increased cell senescence upon the silencing of Ctr9 (Fig. 2F). Ctr9 knockdown also dramatically inhibited MCF7 cell proliferation (Fig. 2G) and colony formation (Fig. 2H),

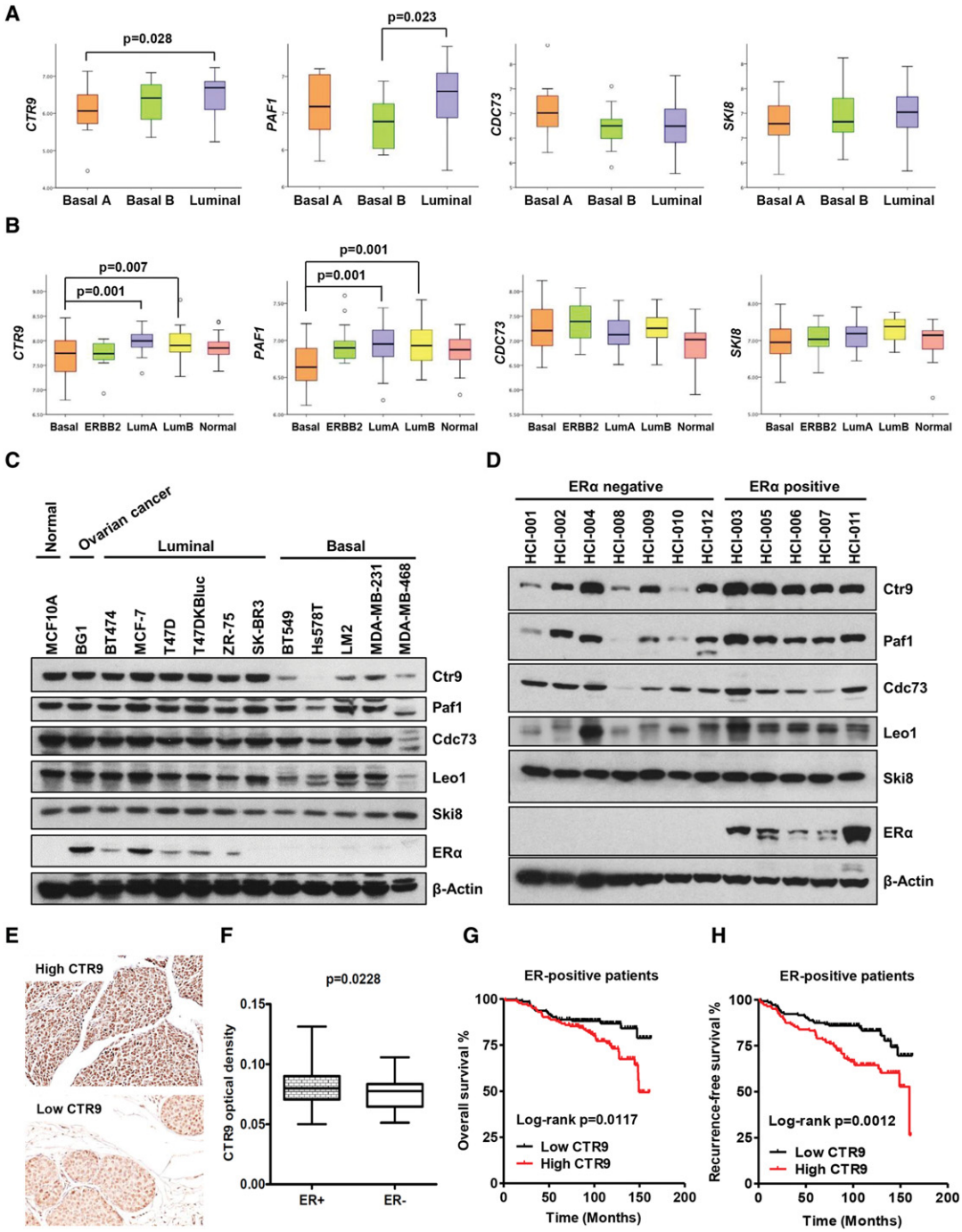

Figure 1. Ctr9 is enriched in ERα+ luminal breast cancer, and high Ctr9 expression correlates with poor prognosis of ERα+ breast cancers. (*A*) Box plots displaying PAFc subunit mRNA levels in basal A ($n = 12$), basal B ($n = 14$), and luminal ($n = 25$) subtypes of breast cancer cell lines using the published microarray data set. *Leo1* is not available in this data set. (*B*) Box plots displaying PAFc subunit mRNA levels in basal-like, ERBB2+, luminal A, luminal B, and normal-like subtypes of breast tumors using the published microarray data set. *Leo1* is not available in this data set. (*C*) Protein levels of PAFc subunits and ERα were examined by Western blots using a series of cell lines, including an immortalized nontransformed mammary epithelial cell line (MCF10A), an ovarian cancer cell line (BG1), six luminal human breast cancer cell lines, and five basal-like human breast cancer cell lines. β-Actin was used as a loading control. (*D*) Protein levels of PAFc subunits and ERα were quantified by Western blots using protein extracts from seven ERα-negative and five ERα-positive patient-derived tumor grafts. β-Actin was used as a loading control. (*E*) Representative images of high and low Ctr9 immunohistochemistry (IHC) staining in the human breast cancer tissue microarray (TMA). (*F*) Box plots displaying Ctr9 expression (optical density) in ERα-positive ($n = 280$) and ERα-negative ($n = 80$) patient samples on the TMA. (*G*,*H*) Kaplan-Meier survival analyses of ERα-positive breast cancer patients depicting the probability of overall (*G*) and recurrence-free (*H*) survival. Patients were stratified on the median value for Ctr9 IHC staining optical density (low Ctr9, $n = 140$; high Ctr9, $n = 140$). The log-rank test *P*-values are shown.

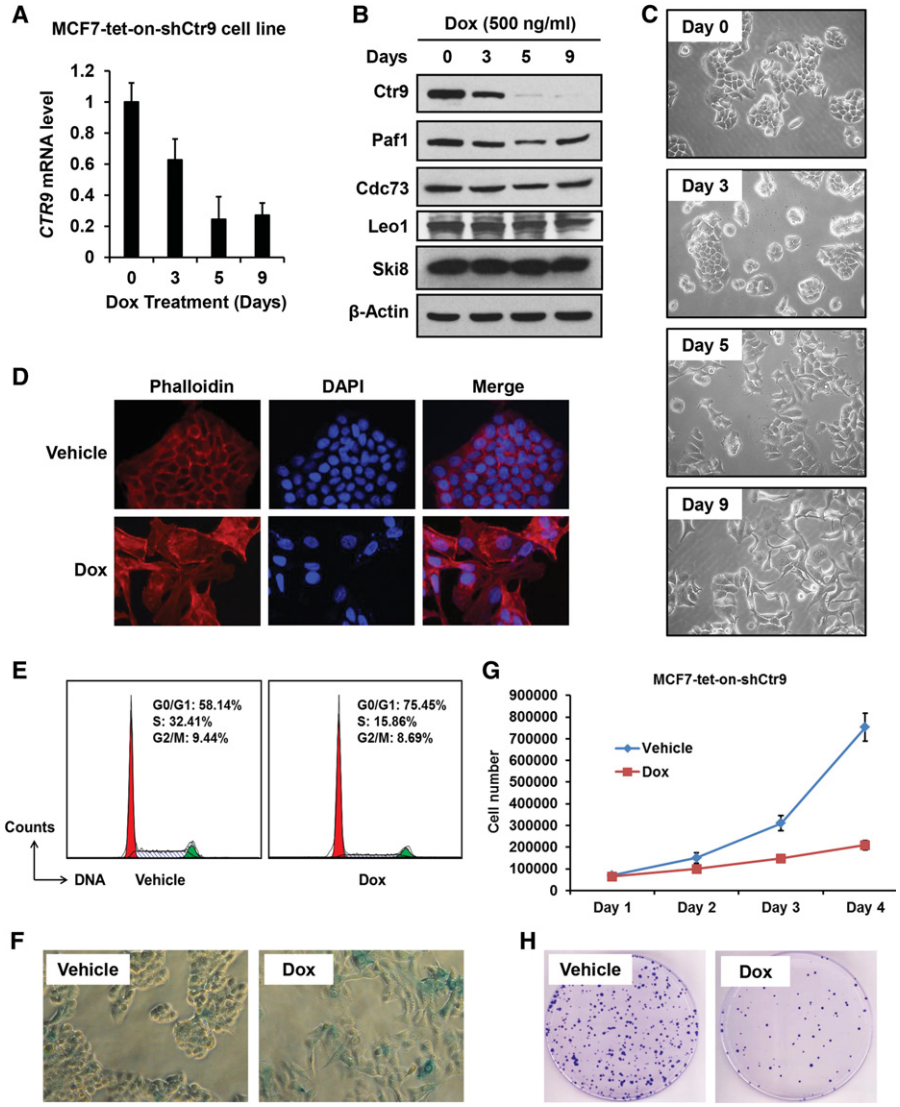

Figure 2. Knockdown of Ctr9 in MCF7 cells leads to morphological change, cell cycle arrest, and growth inhibition. (*A*) Real-time quantitative PCR (qPCR) analyses of *CTR9* mRNA. MCF7-tet-on–shCtr9 cells were treated with 500 ng/mL Dox for the indicated number of days. The mean mRNA levels were normalized to the internal control gene β-Actin and are represented ±SD. $n = 3$. (*B*) Western blot analyses of PAFc subunits. MCF7-tet-on–shCtr9 cells were treated with 500 ng/mL Dox for the indicated number of days. β-Actin was used as a loading control. (*C*) Representative images of cell morphology. MCF7-tet-on–shCtr9 cells were treated with 500 ng/mL Dox for the indicated number of days. (*D*) Alexa fluor 555 phalloidin staining (red) images of MCF-tet-on–shCtr9 cells treated with vehicle or Dox for 9 d. DAPI was used to stain nuclei (blue). (*E*) Cell cycle profiles of vehicle- and Dox-treated MCF7-tet-on–shCtr9 cells assessed by propidium iodide (PI) staining and fluorescence-activated cell scanning (FACS). (*F*) Representative cell images showing the senescence-associated β-galactosidase staining (light blue) on vehicle- or Dox-treated MCF7-tet-on–shCtr9 cells. (*G*) Growth curves of vehicle- or Dox-treated MCF7-tet-on–shCtr9 cells. Cells were pretreated with vehicle or 500 ng/mL Dox for 4 d prior to seeding into six-well plates for cell proliferation assay assessed by cell counting. Data are represented as mean ± SD. $n = 3$. (*H*) Representative images of two-dimensional (2D) colony formation from vehicle- or Dox-treated MCF7-tet-on–shCtr9 cells. Colonies were stained with 0.05% crystal violet.

while Dox elicited no effect on MCF7-tet-on parental cell proliferation (Supplemental Fig. S3B). Moreover, Ctr9 knockdown in MCF7-tet-on–shCtr9 cells grown in estrogen-deprived medium had little if any effect on cell proliferation (Supplemental Fig. S3E), indicating that the effect of Ctr9 knockdown on cell proliferation is estrogen-dependent.

To rule out the possibility that the results reflect off-target effects of Ctr9 shRNA, similar experiments were performed using MCF7 cells stably expressing two distinct, lentiviral Ctr9 targeted shRNAs (shCtr9 #3 and #5). In these cells, Ctr9 protein was undetectable by Western blot (Supplemental Fig. S5A, lanes 1–3), and expression of the other four subunits in hPAFc was significantly reduced, consistent with the previous reports (Youn et al. 2007; Wu and Xu 2012). Similar to the inducible Ctr9 knockdown, stable Ctr9 knockdown in MCF7 cells also triggered dramatic morphological changes (Supplemental

Fig. S4A) and cell growth defects (Supplemental Fig. S4B). Similar experiments were also performed using ERα+ luminal breast cancer cell line T47D (Supplemental Fig. S4D), and similar results were observed, including morphological changes (Supplemental Fig. S4C) and impaired cell growth (Supplemental Fig. S4E). Collectively, these data suggest that Ctr9 plays a role in ERα+ breast cancer cell growth.

hPAFc is a multiprotein complex composed of the Ctr9, Paf1, Cdc73, Leo1, and Ski8 subunits. However, several lines of evidence suggest that some hPAFc subunits play roles that are independent of hPAFc (Chaudhary et al. 2007). To determine whether silencing of other subunits of hPAFc causes similar effects, MCF7 cells were infected by lentiviral shRNA constructs targeting other hPAFc subunits, stable knockdown cell lines were isolated, and the knockdown efficiency was determined by Western blot (Supplemental Fig. S5A). The Western blot data indicate that expression of Cdc73, Ski8, and Ctr9 was reduced to similar low percentages of wild-type expression, while Leo1 was only partially knocked down, and Paf1 expression was not reduced significantly for any of the several shRNAs tested. Surprisingly, cell morphology and cell growth were normal (i.e., no different from MCF7 control cells) in cells knocked down for other subunits of hPAFc (Supplemental Fig. S5B,C), indicating that Ctr9 is the key subunit in hPAFc that regulates the proliferation and morphology of ERα+ luminal breast cancer cells. This function could be intrinsic to Ctr9 alone or in complex with other subunits in PAFc.

The role of Ctr9 in ERα− basal-like cells was examined in a similar manner, infecting ERα− MDA-MB-231 cells with lentivirus encoding Ctr9 targeted shRNA (Supplemental Fig. S6A). Unlike the results in ERα+ cells, Ctr9 knockdown exhibited no effects on the cell morphology, cell growth, and colony formation of MDA-MB-231 cells (Supplemental Fig. S6B–D). This could reflect the fact that Ctr9 expression is generally low in ERα− basal-like breast cancer cells (Fig. 1); however, the effects of knocking down Ctr9 may be subtler in ERα− cells than ERα+ cells, and, to detect them, a gain-of-function approach may be informative. However, overexpression of Ctr9 in MDA-MB-231 cells also had no effects on cell morphology, cell growth, or colony formation (Supplemental Fig. S6E–H). Collectively, these results suggest that Ctr9 plays a tumorigenic role specifically in ERα+ luminal breast cancer cells, which is consistent with the higher level of expression of Ctr9 in these cells.

Knockdown of Ctr9 increases sensitivity of ERα+ luminal breast cancer cells to tamoxifen

Because ERα+ luminal breast tumors depend on ERα for growth, the ERα antagonist tamoxifen is commonly used to treat ERα+ cancers. However, in many cases, the efficacy of tamoxifen decreases over time of treatment. Because Ctr9 appears to play a critical role during proliferation of ERα+ luminal breast cancer, we hypothesized that loss of Ctr9 might act synergistically with tamoxifen to inhibit ERα-dependent cancer cell growth. Indeed, increasing doses of 4-hydroxylated tamoxifen (4-OHT) resulted in more pronounced cell growth defects in Ctr9 knockdown MCF7 cells (Fig. 3A). To better understand the mechanisms underlying acquired tamoxifen resistance in ERα+ luminal breast cancer cells, we used estrogen-independent (MCF7/LCC1) and tamoxifen-resistant (MCF7/LCC2) cell lines that were previously established by long-term estrogen deprivation and stepwise tamoxifen selection against parental MCF7 cells (Jørgensen et al. 1997), respectively. Western blotting showed that expression of Ctr9, but not the other subunits of hPAFc, was increased along with the acquisition of tamoxifen resistance (Fig. 3B). Notably, ERα was also more abundant in MCF7/LCC1 and MCF7/LCC2 cell lines (Fig. 3B). To evaluate whether the higher Ctr9 expression in tamoxifen-resistant MCF7/LCC2 cells is functionally important, we knocked down Ctr9 in MCF7/LCC2 cells and assessed cell growth and colony formation (Fig. 3C,D). Ctr9 knockdown significantly inhibited the growth and colony formation of MCF7/LCC2 cells. Importantly, Ctr9 knockdown triggered a greater fold reduction in cell growth and colony formation in the presence of 4-OHT compared with the dimethyl sulfoxide (DMSO) control (Fig. 3C,D, cf. the third and fourth bars), indicating the gain of sensitivity to tamoxifen treatment in Ctr9-depleted MCF7/LCC2 cells. Similar results were also obtained when Ctr9 was knocked down in intrinsically tamoxifen-resistant BT474 cells (Supplemental Fig. S7A–C). To evaluate whether Ctr9 abundance has potential clinical significance as a correlate of tamoxifen sensitivity, a subset ($n = 239$) of the ERα+ breast cancer patients analyzed in Figure 1, E–H, were stratified by Ctr9 abundance and their survival curves after tamoxifen chemotherapy. Kaplan-Meier survival analyses showed a significant correlation between high Ctr9 expression ($n = 120$) and poor overall and recurrence-free survival (Fig. 3E,F), suggesting that high Ctr9 expression is associated with poor response to tamoxifen adjuvant chemotherapy.

Ctr9 serves as a central regulator of estrogen signaling

To better understand the role of Ctr9 in ERα+ breast tumorigenesis, human transcriptome analysis was performed in MCF7-tet-on–shCtr9 cells treated with vehicle or Dox followed by DMSO or E2 treatment (Supplemental Fig. S8B,C). Differentially expressed genes were identified, and the data are presented in a heat map in Figure 4A using a 1.5-fold change in relative expression level as a cutoff for significance (false discovery rate [FDR] < 0.05). We note that exposure to E2 does not affect any of the hPAFc subunits (Supplemental Fig. S8A). To identify transcriptomes regulated by E2 and Ctr9, we performed four comparisons as shown in Figure 4B. This analysis identified 1603 E2-responsive genes (vehicle E2 vs. vehicle DMSO), only 57 of which remained responsive to E2 after Ctr9 knockdown (Dox E2 vs. Dox DMSO). A Venn diagram analysis suggests that the majority of E2-responsive genes, either activated or repressed, lost their responsiveness to E2 in the absence of Ctr9 (Fig. 4C), confirming the conclusion that Ctr9 is indispensable for E2-regulated gene transcription.

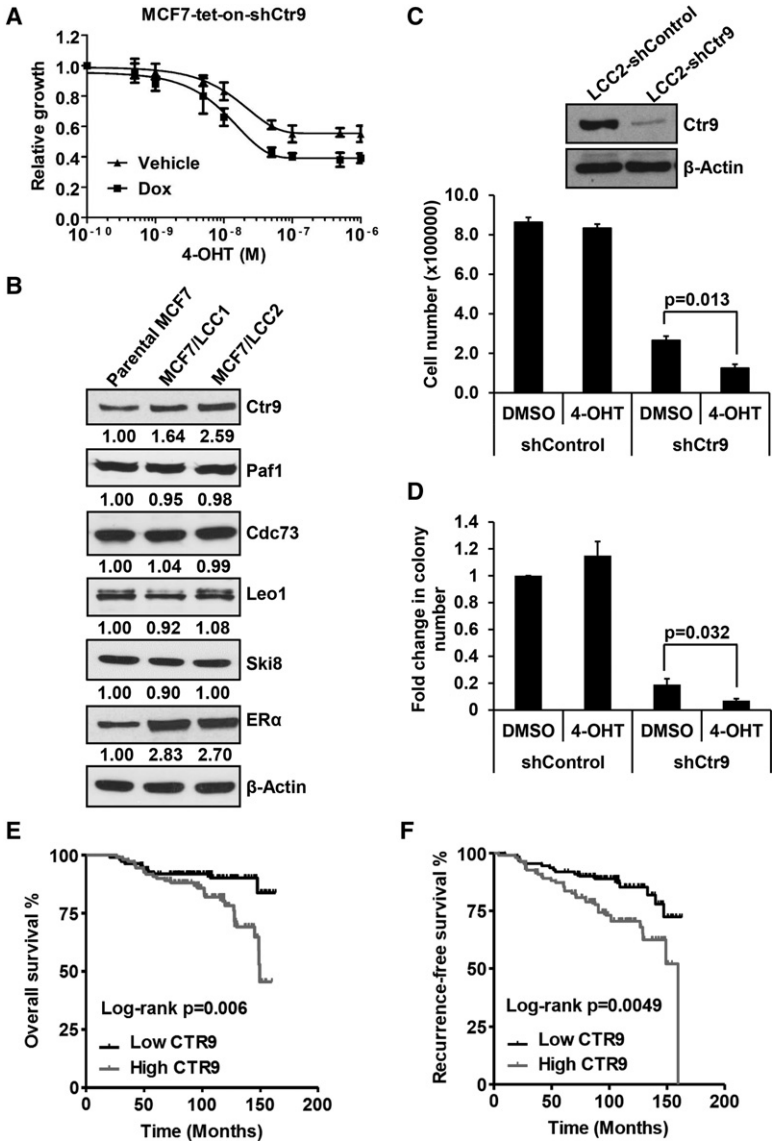

Figure 3. High Ctr9 expression in tamoxifen-resistant cells influences proliferation and colony formation, and high Ctr9 expression in tamoxifen-treated patients correlates with poor survival. (*A*) 4-OHT dose-responsive growth curve measured by 3-(4,5-dimethylthiazol-2-yl)-2,5-diphenyltetrazolium (MTT) assay in MCF7-tet-on–shCtr9 cells treated with vehicle or Dox. Data are mean ± SD ($n = 3$) normalized to 10^{-10} M 4-OHT treatment data. (*B*) Western blot of PAFc subunits and ERα in parental MCF7, estrogen-independent MCF7/LCC1, and tamoxifen-resistant MCF7/LCC2 cell lines. β-Actin was used as a loading control. Quantification of PAFc subunits and ERα was done using ImageJ and normalized to β-Actin; values in parental MCF7 cells were set to 1. (*C*) Measurement of cell proliferation by cell counting in control or Ctr9 knockdown MCF7/LCC2 cells treated with DMSO control or 1 µM 4-OHT for 4 d. Data are represented as mean ± SD. $n = 3$. Ctr9 knockdown efficiency was determined by Western blot, and β-Actin was used as a loading control. (*D*) Measurement of 2D colony formation in control or Ctr9 knockdown MCF7/LCC2 cells treated with DMSO control or 1 µM 4-OHT for 2 wk. Colonies were stained with 0.05% crystal violet, and colony number was counted using ImageJ software. Data are represented as mean ± SD ($n = 3$) and were normalized to the shControl_DMSO treatment group. (*E*,*F*) Kaplan-Meier survival analyses of tamoxifen-treated ERα-positive breast cancer patients depicting the probability of overall (*E*) and recurrence-free (*F*) survival. Patients were stratified on the median value for Ctr9 IHC staining optical density on the breast cancer TMA (low Ctr9, $n = 119$; high Ctr9, $n = 120$). The log-rank test *P*-values are shown.

In fact, Ctr9 knockdown in the absence of E2 affected more genes than Ctr9 knockdown in the presence of E2 (Fig. 4B), and these genes were either E2-dependent or E2-independent (Fig. 4D; Supplemental Fig. S8D). Pathway analyses of genes in the Ctr9-regulated transcriptome revealed that Ctr9 primarily modulates the expression of genes that regulate cell death and survival, cell movement, cellular growth and proliferation, and cell morphology (Supplemental Figs. S9, S10), which is consistent with the results presented above (Fig. 2). To validate this human transcriptome analysis, quantitative RT–PCR (qRT–PCR) analyses were performed for selected Ctr9 target genes—including up-regulated genes (Fig. 4E), down-regulated non-estrogen-responsive genes (Fig. 4F), and down-regulated estrogen-responsive genes—upon silencing of Ctr9 (Fig. 4G). Importantly, these genes have been previously reported to have roles in ERα$^+$ breast tumorigenesis and/or endocrine resistance. Consistent with the hPAFc-independent role of Ctr9 in driving ERα$^+$ cell growth, none of the Ctr9 target genes was affected by the loss of the other individual subunits in hPAFc (Supplemental Fig. S8E–G). Collectively, these data substantiate Ctr9 as a central regulator of estrogen signaling in ERα$^+$ breast cancer cells.

Knockdown of Ctr9 decreases ERα protein level and stability

Because ERα is the key determinant of estrogen signaling, we examined whether Ctr9 regulates ERα itself. Indeed, although the *ESR1* mRNA level was not affected by Ctr9 knockdown (Supplemental Fig. S11), the ERα protein level was dynamically changed by the addition and withdrawal of Dox, mirroring the expression pattern of Ctr9 in MCF7-tet-on–shCtr9 cells (Fig. 5A). In contrast, the ERα protein level was not affected by Dox in MCF7-tet-on parental cells (Supplemental Fig. S3A). The reduction of the ERα protein level was more pronounced in

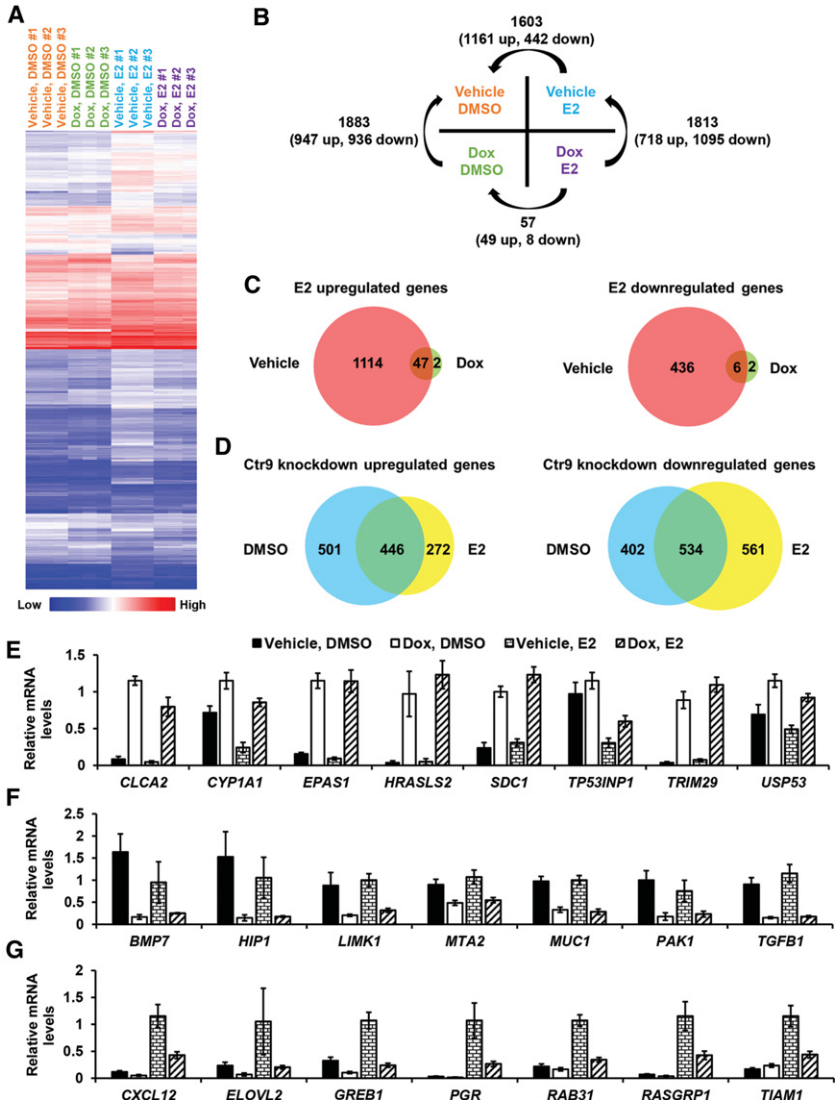

Figure 4. Global identification of estrogen- and Ctr9-regulated transcriptomes in MCF7-tet-on–shCtr9 cells using human transcriptome arrays. (*A*) Heat map generated from Affymetrix human transcriptome array 2.0 analysis of triplicate samples of MCF7-tet-on–shCtr9 cells treated with vehicle or Dox followed by DMSO control or 10 nM E2 (4 h) treatment. Differentially expressed genes with >1.5-fold change and FDR <0.05 are shown. (*B*) A matrix describing the approach used to identify differentially expressed genes. (*C*) Venn diagrams showing the overlaps between E2 up-regulated (*left*) or E2 down-regulated (*right*) genes identified in control and Ctr9 knockdown conditions. (*D*) Venn diagrams showing the overlaps between Ctr9 knockdown up-regulated (*left*) or Ctr9 knockdown down-regulated (*right*) genes identified in DMSO control and 10 nM E2-treated conditions. (*E–G*) Measurements of Ctr9 target gene expression by real-time qPCR for selected up-regulated genes (*E*), down-regulated non-estrogen-responsive genes (*F*), and down-regulated estrogen-responsive genes (*G*) upon silencing of Ctr9. mRNA levels are represented as means ± SD ($n = 3$) and were normalized to the internal control gene β-Actin.

MCF7 cells stably knocked down for Ctr9 (Supplemental Fig. S5A), and a similar effect was observed in T47D cells (Supplemental Fig. S4D). In addition, E2-induced proteasome-dependent degradation of ERα was enhanced by Ctr9 knockdown, which can be partially blocked by the proteasome inhibitor MG132 (Fig. 5B). In line with this finding, Ctr9 knockdown significantly increased ubiquitination of ERα (Fig. 5C) and decreased its stability (Fig. 5D). Despite this, Ctr9 knockdown did not affect the nuclear localization of ERα (Fig. 5E). Therefore, we propose that Ctr9 regulates ERα in a post-translational manner. The latter hypothesis is consistent with the fact that knockdown of Ctr9 correlates with lower abundance of endogenous ERα and exogenous Flag-ERα in MCF-tet-on–shCtr9 cells engineered to overexpress Flag-ERα (Fig. 5F). Although overexpression of ERα failed to rescue the morphological change triggered by Ctr9 knockdown (Fig. 5G), the growth defect resulting from Ctr9 knockdown was partially rescued by overexpression of ERα (Fig. 5H). Moreover, overexpression of ERα restored a normal expression level to some but not all mRNAs differentially affected by Ctr9 knockdown (Fig. 5I). Altogether, these data suggest that Ctr9 enhances ERα protein stability and that loss of Ctr9 suppresses signaling through ERα to downstream targets. To gain additional insight into how Ctr9 regulates ERα protein stability, we observed that Ctr9 knockdown significantly decreased the expression of the *MUC1* gene (Fig. 4F). *MUC1* encodes Mucin 1 (MUC1), a tumor-associated glycoprotein that is overexpressed in breast cancer and is associated with poor prognosis (Hattrup and Gendler 2006). The MUC1 C-terminal subunit (MUC1-C) has been shown to bind directly to ERα and stabilize ERα protein by blocking its ubiquitination and degradation (Wei et al. 2006). Western blot analyses confirmed that MUC1-C protein was significantly decreased by knockdown of Ctr9 but not other PAFc subunits, and the reduced MUC1-C protein level can be recovered by restoring Ctr9 expression (Supplemental Figs. 12A–C). Moreover, coimmunoprecipitation (co-IP) experiments showed that Ctr9 knockdown reduced the amount of

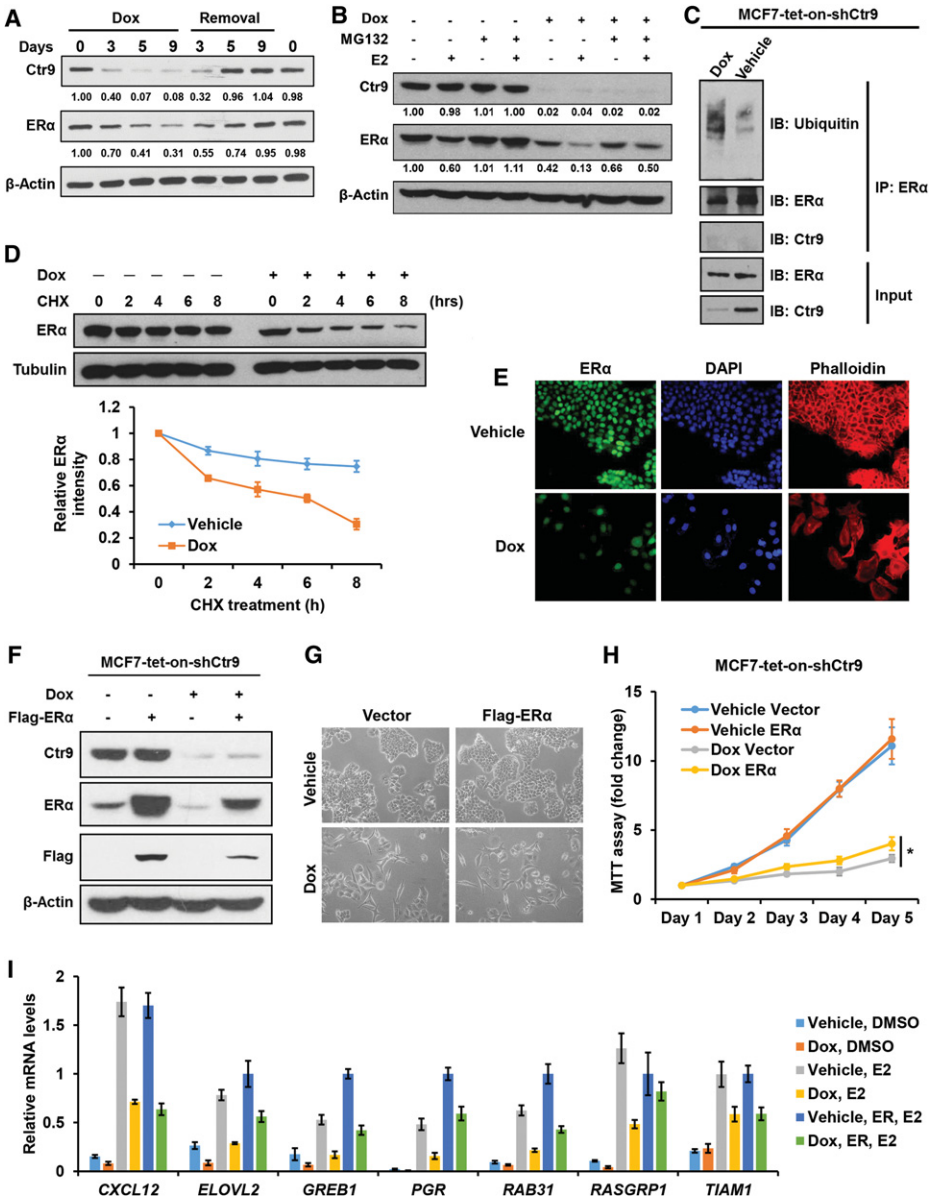

Figure 5. Knockdown of Ctr9 decreases ERα protein level and stability. (*A*) Western blot analyses of Ctr9 and ERα. MCF7-tet-on–shCtr9 cells were cultured in medium containing 500 ng/mL Dox for 0, 3, 5, and 9 d; transferred to fresh cell culture medium lacking Dox; and cultured for an additional 3, 5, and 9 d. β-Actin was used as a loading control. Quantification of Ctr9 and ERα was done using ImageJ and normalized to β-Actin; values in vehicle-treated MCF7-tet-on–shCtr9 cells (day 0) were set to 1. (*B*) Western blot analyses of Ctr9 and ERα in MCF7-tet-on–shCtr9 cells in response to Ctr9 knockdown (500 ng/mL Dox treatment), 10 nM E2 induction for 2 h, and 10 µM MG132 proteasome inhibitor treatment for 2 h. β-Actin was used as a loading control. Quantification of Ctr9 and ERα was performed using ImageJ and normalized to β-Actin; values in control cells (vehicle-treated; the first lane) were set to 1. (*C*) Detection of in vivo ubiquitinated ERα by immunoblotting of ERα immunoprecipitates with anti-ubiquitin antibody in vehicle- or Dox-treated MCF7-tet-on–shCtr9 cells. Western blots of Ctr9 and ERα are also shown. (*D*) Measurement of ERα protein stability. Vehicle- or Dox-treated MCF7-tet-on–shCtr9 cells were treated with cycloheximide (CHX; 50 µg/mL final concentration) for the indicated time points followed by Western blot analysis of ERα. Quantification of ERα was done using ImageJ and normalized to tubulin; values in control conditions (CHX, 0 h of treatment) were set to 1. Data are represented as mean ± SD. $n = 3$. (*E*) Immunofluorescence staining of ERα (green) in vehicle- or Dox-treated MCF7-tet-on–shCtr9 cells depicting that knockdown of Ctr9 does not affect ERα nuclear localization. Nuclei and F-Actin were visualized by DAPI (blue) and phalloidin (red) staining, respectively. (*F*) Western blot analyses of Ctr9 and ERα in vehicle- or Dox-treated MCF7-tet-on–shCtr9 cells infected with vector or Flag-ERα-expressing retrovirus. Exogenous Flag-ERα was immunoblotted with anti-ERα and anti-Flag antibodies. β-Actin was used as a loading control. (*G*) Representative morphology images of MCF7-tet-on–shCtr9 cells treated as in *F*. (*H*) Cell proliferation of MCF7-tet-on–shCtr9 cells treated as in *F* was determined by MTT assays. Data are represented as mean ± SD. $n = 3$. (*) $P < 0.05$. (*I*) Real-time qPCR analyses of mRNA levels of Ctr9-regulated estrogen-responsive genes in vehicle- or Dox-treated MCF7-tet-on–shCtr9 cells infected with vector or Flag-ERα-expressing retrovirus followed by DMSO or 10 nM E2 induction for 4 h. Data are represented as mean ± SD ($n = 3$) and were normalized to internal control gene β-Actin.

MUC1-C protein binding to ERα (Supplemental Fig. 12D). Therefore, these results provided a possible mechanism by which Ctr9 affects ERα protein stability, involving the Ctr9–MUC1–ERα cascade.

Recent evidence shows that E2 rapidly activates cytosolic kinase signaling pathways by triggering the formation of cytoplasmic ERα-containing complexes that mediate rapid changes in cell morphology, cell growth, and endocrine responsiveness. Here we explored a possible role for Ctr9 in E2-mediated effects on extranuclear kinase signaling pathways of ERα. Total and activated/phosphorylated forms of MAPK and Akt were assessed by Western blots with or without knockdown of Ctr9. The results confirmed that Ctr9 knockdown decreases activation of extranuclear kinase in MCF7 cells (Supplemental Fig. S13). Collectively, these findings demonstrate that Ctr9 regulates both nuclear and extranuclear ERα-dependent signaling; hence, loss of Ctr9 has a dramatic effect on the growth and morphology of ERα+ breast cancer cells.

Ctr9 regulates estrogen-stimulated transcription by controlling ERα and RNAPII occupancy, histone H2Bub1, and transcription elongation

The data presented above show that knockdown of Ctr9 alters the transcription of E2-responsive genes (Fig. 4) and decreases the level of ERα protein (Fig. 5). Therefore, we surmised that the chromatin-associated fraction of ERα would decrease when Ctr9 is silenced. Indeed, chromatin immunoprecipitation (ChIP) assays revealed that E2 treatment significantly enhanced the occupancy of Ctr9 (Fig. 6A) and ERα (Fig. 6B) on estrogen response elements (EREs) of *CXCL12*, *GREB1*, and *PGR* genes selected from the microarray data, confirming that these genes are direct targets of Ctr9 and ERα. More importantly, knockdown of Ctr9 dramatically reduced E2-enhanced binding of Ctr9 (Fig. 6A) and ERα (Fig. 6B) to ERE regions. In keeping with this finding, E2-enhanced RNAPII occupancy on the same ERE regions of *CXCL12*, *GREB1*, and *PGR* genes was also significantly decreased by Ctr9 knockdown (Fig. 6C,D), suggesting that loss of Ctr9 affects transcription initiation of ERα target genes by interfering with recruitment of ERα and RNAPII. In response to E2 treatment, ERα recruits various cofactors to deposit active histone marks; i.e., histone H3 acetylation catalyzed by p300/CBP. Indeed, accompanied by the decreased ERα occupancy upon Ctr9 silencing, H3K27ac ChIP assays revealed reduction of H3K27ac near the transcription start sites (TSSs) of *CXCL12*, *GREB1*, and *PGR* genes (Fig. 6E), although the global distribution of H3K27ac was unaffected (Fig. 6F). Because Ctr9 plays well-established roles in controlling transcription elongation and transcription-coupled histone modifications (Crisucci and Arndt 2011; Tomson and Arndt 2013), we examined the effects of Ctr9 knockdown on transcriptional elongation by RNAPII and the coupled incorporation of H2Bub1 in ERα+ breast cancer cells. Interestingly, Western blot analyses of the whole-cell lysates of MCF7-tet-on–shCtr9 cells revealed that E2 treatment substantially increased bulk levels of RNAPII pSer2 and H2Bub1, while Ctr9 knockdown decreased E2-induced RNAPII pSer2 as well as basal and E2-induced H2Bub1 (Fig. 6F). Moreover, two other histone modifications associated with the active transcription, H3K4me3 and H3K36me3, were also decreased in the bulk level upon loss of Ctr9 (Fig. 6F). A more robust effect on these histone modifications was observed in MCF7 cells with stable Ctr9 knockdown (Supplemental Fig. S14A,B), while changes in histone modifications were not detected upon stable knockdown of other PAFc subunits (Supplemental Fig. 14B,C). Consistent with the global effect, ChIP assays on the transcribed regions (TRs) of *CXCL12*, *GREB1*, and *PGR* genes further revealed that Ctr9 knockdown significantly decreased the occupancy of Ctr9, H2Bub1, and RNAPII pSer2 in E2-treated cells (Fig. 6G–J). Given that ERα interacts with the positive transcription elongation factor-b (P-TEFb) complex that promotes transcriptional elongation in part by relieving the negative elongation factor (NELF) complex and stimulating RNAPII pSer2 (Wittmann et al. 2005; Peterlin and Price 2006), which in turn promotes elongation-associated histone modifications (Pirngruber et al. 2009), we further performed ChIP assays for CDK9 and NELF-A and observed that Ctr9 knockdown decreased the occupancy of CDK9 and increased the occupancy of NELF-A at *CXCL12*, *GREB1*, and *PGR* genes (Supplemental Fig. S15A–C). Collectively, these data demonstrate that loss of Ctr9 has multifaceted effects on the estrogen-regulated transcriptional program by destabilizing ERα, reducing ERα and RNAPII occupancies on chromatin, and affecting transcription elongation and elongation-coupled histone modifications (Fig. 7). This study suggests a more extensive and more important role for Ctr9 in transcriptional regulation of ERα than previously thought.

Discussion

The major finding of this study is that Ctr9, a key subunit of hPAFc, regulates multiple steps in ERα-dependent transcription: controlling ERα stability as well as promoting transcriptional elongation (Fig. 7). The ability of Ctr9 to stimulate E2-ERα-dependent transcription could potentially explain its proproliferative effect on cancer cells as well as the correlation between high Ctr9 expression and poor survival outcome in ERα+ breast cancer patients and resistance to tamoxifen in ERα+ breast cancer cells. The ability of Ctr9 to block G1 cell cycle arrest in MCF7 cells appears to be evolutionarily conserved in that yeast Ctr9 positively regulates expression of G1 cyclin (Koch et al. 1999). These results suggest that Ctr9 could be considered a master regulator of ERα-dependent transcription and plays a critical role in the progression and pathogenesis of ERα+ luminal breast cancer. Additional studies are needed to determine whether Ctr9 is a useful prognostic marker for resistance to tamoxifen.

The gene expression analyses presented here demonstrate that knockdown of Ctr9 in MCF7 cells strongly suppresses global estrogen signaling and interferes with induction of E2-responsive genes. In addition, this effect

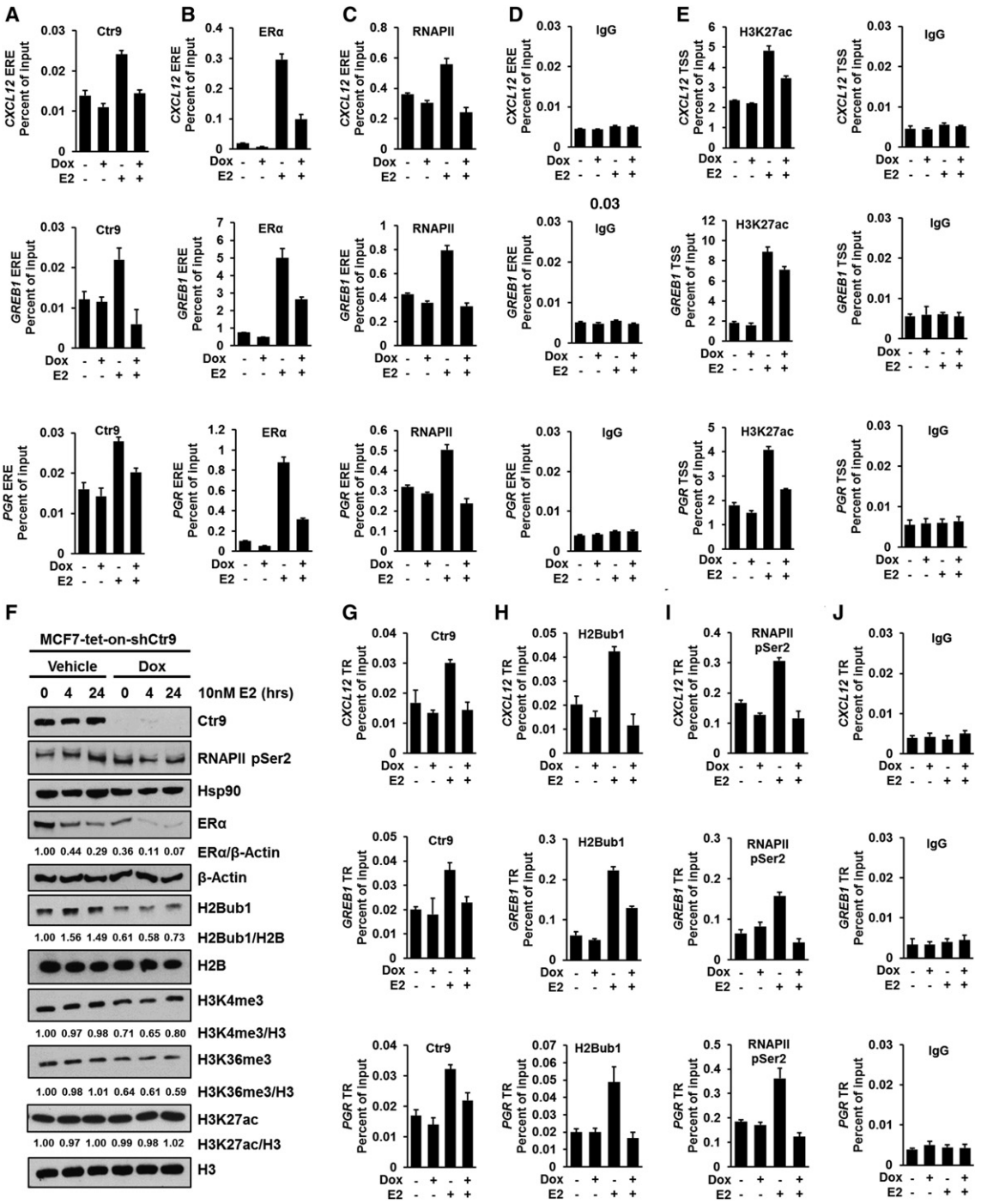

Figure 6. Ctr9 regulates estrogen-stimulated transcription by controlling the occupancy of ERα and RNAPII and the accumulation of histone H2Bub1 and the elongated form of RNAPII at estrogen-responsive genes. (*A–D*) ChIP-qPCR analyses of the occupancy of Ctr9 (*A*), ERα (*B*), RNAPII (*C*), and IgG control (*D*) on the EREs of ERα target genes (*CXCL12*, *GREB1*, and *PGR*) in MCF7-tet-on–shCtr9 cells treated with vehicle or 500 ng/mL Dox followed by DMSO or 10 nM E2 induction for 45 min. (*E*) ChIP-qPCR analyses of the occupancy of H3K27ac near the TSSs of *CXCL12*, *GREB1*, and *PGR* genes in MCF7-tet-on–shCtr9 cells treated with vehicle or 500 ng/mL Dox followed by DMSO or 10 nM E2 induction for 45 min. IgG was used as a negative control. (*F*) Western blot analyses with specific antibodies on whole-cell lysates of MCF7-tet-on–shCtr9 cells treated with vehicle or 500 ng/mL Dox followed by 10 nM E2 induction for 0, 4, or 24 h. Relative quantified values of ERα normalized to β-Actin, H2Bub1 normalized to H2B, H3K4me3 normalized to H3, H3K36me3 normalized to H3, and H3K27ac normalized to H3 are indicated *below* the respective blots. (*G–J*) ChIP-qPCR analyses of the occupancy of Ctr9 (*G*), H2Bub1 (*H*), RNAPII pSer2 (*I*), and IgG control (*J*) on the TRs of *CXCL12*, *GREB1*, and *PGR* genes in MCF7-tet-on–shCtr9 cells treated with vehicle or 500 ng/mL Dox followed by DMSO or 10 nM E2 induction for 45 min. ChIP-qPCR data were normalized to input DNA qPCR data and expressed as "percent of input"; data are represented as mean ± SD. $n = 3$.

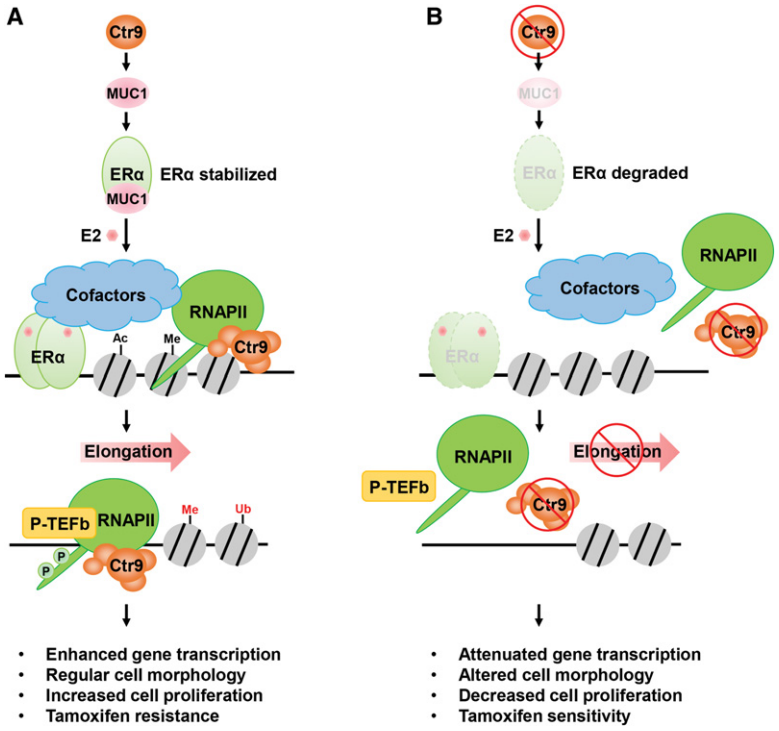

Figure 7. Model depicting the roles of Ctr9 in regulating ERα-dependent transcription and cellular effects. (*A*) Ctr9 controls the expression of MUC1 at the mRNA and protein levels. The MUC1 C terminus binds directly to ERα and stabilizes ERα protein by blocking its ubiquitination and degradation. Upon E2 binding, ERα dimers associate with the EREs on chromatin, where it recruits coactivators to modify histones by acetylation and methylation, leading to further recruitment of the downstream effectors and RNAPII. The P-TEFb complex phosphorylates Ser2 within the C-terminal domain of RNAPII, leading to efficient transcription elongation as well as elongation-associated histone modifications such as H2Bub1 and H3K36me3. The coordinated transcriptional program enhances the expression of ER target genes that are responsible for maintaining cell morphology, accelerating cell proliferation, and acquiring tamoxifen resistance in ERα-positive breast cancer cells. (*B*) Knockdown of Ctr9 decreases MUC1 and ERα protein, resulting in reduction of ERα transcriptional complex assembly, transcriptional elongation, and transcription-coupled histone modifications. As a consequence of the attenuated ERα transcriptional program, the ER target gene expression, cell morphology, cell proliferation, and tamoxifen sensitivity are changed correspondingly.

was partially rescued by overexpression of ERα. Interestingly, Ctr9 promotes expression of *GREB1*, one of the genes most strongly induced by estrogen. GREB1 was recently identified as the estrogen-specific ERα interactor, which is essential for ERα-mediated transcription and growth in ERα⁺ breast cancer cells (Mohammed et al. 2013). Ctr9 also stimulates ERα-dependent transcription of LIMK1, PAK1, and TIAM1—proteins that regulate actin dynamics and the maintenance of cell morphology (Jiang et al. 2009). The fact that Ctr9-dependent expression of genes is involved in actin organization is consistent with a recent report that a PAF1–ERK5–ERα complex plays a role in actin reorganization via regulation of a transcriptional program of ERα in breast cancer (Madak-Erdogan et al. 2014). PAFc has been previously shown to facilitate transcription elongation and transcription-coupled histone modifications (Tomson and Arndt 2013), including H2Bub1, which is required for ERα-regulated gene transcription (Prenzel et al. 2011). Consistent with these reports, we demonstrated that Ctr9 promotes E2-stimulated transcription initiation by stimulating recruitment of ERα and RNAPII to target promoters and promoting downstream H3K27ac. Ctr9 also appears to stimulate deposition of transcription elongation-associated RNAPII pSer2, H2Bub1, and H3K36me3. In conclusion, our study elucidates the multifaceted roles of Ctr9 in regulation of ERα-dependent transcription. Another unexpected finding of our study is that Ctr9 also regulates an ERα extranuclear kinase signaling pathway through MAPK and AKT that also plays significant roles in the proliferation of ERα⁺ breast cancer cells and tamoxifen resistance (Levin 2005). A previous report demonstrated that methylation of ERα by PRMT1 is required for the rapid kinase cascade transduction of estrogen signaling (Le Romancer et al. 2008). Interestingly, PRMT1 expression decreases when Ctr9 is knocked down (data not shown). Therefore, Ctr9 might modulate the ERα-dependent extranuclear kinase signaling by stabilizing ERα and promoting expression of PRMT1, which in turn would increase methylation of ERα.

Tamoxifen is the first-line treatment for patients with ERα⁺ breast cancer (Cleator et al. 2009). However, it is common that tumors develop de novo or acquired resistance to endocrine therapy owing to the dysregulation of the ERα protein itself or ERα-associated factors (Droog et al. 2013). For example, loss of LMTK3, a positive regulator of ERα protein, can revert the tamoxifen resistance in cell line models (Giamas et al. 2011). Interestingly, knockdown of Ctr9 appears to restore tamoxifen sensitivity in ERα⁺ breast cancer cells. Consistent with this, expression of MUC1 and PAK1, two known ERα protein regulators (Rayala et al. 2006b; Wei et al. 2006), decreases upon Ctr9 knockdown. A similar effect was observed with the tamoxifen resistance-associated gene *MTA2* (Rayala et al. 2006a; Pitroda et al. 2009; Bostner et al. 2010; Barone et al. 2011; Kharbanda et al. 2013). However, the mechanism by which Ctr9 regulates tamoxifen resistance is unknown, and it is unclear how Ctr9 expression is up-regulated in tamoxifen-resistant breast cancer cells. Furthermore, we found that knockdown of Ctr9 increased ERα polyubiquitination and decreased ERα protein stability. However, co-IP experiments did not provide evidence that Ctr9 directly interacts with ERα, indicating that Ctr9 post-transcriptionally regulates the ERα protein indirectly. While our finding provided a possible mechanism involving the Ctr9–MUC1–ERα regulatory cascade, we

cannot exclude other mechanisms by which Ctr9 affects ERα protein stability. It also remains unclear whether destabilization of the ERα protein upon loss of Ctr9 is attributed to the tamoxifen sensitization phenotype.

Although the expression of hPAFc subunits is coordinately regulated, the stoichiometry of hPAFc is known to vary in different breast cancer cells and tumors. This suggests that hPAFc stoichiometry could be context-dependent, which is consistent with the idea that Ctr9 and possibly other hPAFc subunits have roles independent of hPAFc. Since Ctr9, but no other hPAFc subunits except Paf1, modulates cell morphology, cell growth, ERα protein stability, and ERα-dependent gene expression, this study suggests a possible hPAFc-independent role for Ctr9 in ERα$^+$ breast cancer. However, our Ctr9 knockdown approach could not distinguish whether Ctr9 functions independently or in the context of PAFc. Although multiple shRNAs against *PAF1* were tested, no conditions were found in which Paf1 expression was strongly inhibited in MCF7 cells. Therefore, we cannot exclude the possibility that both Ctr9 and Paf1 are required for ERα$^+$ breast cancer cell growth. In fact, the functions of Ctr9 and Paf1 are difficult to separate because they share similar expression patterns (Fig. 1), and, in yeast, both Ctr9 and Paf1 are crucial for cell growth (Betz et al. 2002). However, *ctr9*Δ and *paf1*Δ yeast strains exhibited distinct proteome alterations relative to isogenic wild-type yeast cells (Massoni-Laporte et al. 2012). This suggests that Ctr9 and Paf1 might have distinct interacting partners and distinct functions independent of PAFc. In fact, Paf1, but not the other PAFc subunits, plays a significant role in the self-renewal and drug resistance of cancer stem cells (Vaz et al. 2014). The context-dependent stoichiometry of PAFc should be considered when interpreting the functionality of each PAFc subunit. For example, the abundance of yeast Ctr9 is ~10-fold higher than other PAFc subunits and RNAPII, making it the most abundant protein in the yeast nucleus (Mueller et al. 2004). Finally, to explain the unique functional role of Ctr9 in ERα$^+$ breast cancer cells, we postulate that Ctr9 has novel interacting partners in this cellular context. Importantly, Ctr9 protein contains tetratrico peptide repeat (TPR) motifs that are important for protein–protein interaction (Chaudhary et al. 2007; Tomson and Arndt 2013), and germline mutations in the TPR domain of Ctr9 predispose to Wilms tumor (Hanks et al. 2014). Future proteomic studies of Ctr9-interacting proteins in MCF7 cells could provide insight into the mechanisms by which Ctr9 drives ERα$^+$ breast carcinogenesis. Nonetheless, we cannot rule out the possibility that intact hPAFc is required at some level for the full impact of Ctr9 in ERα$^+$ breast cancer because knockdown of Ctr9 at least partially suppresses expression of all PAFc subunits (this study) and disrupts the integrity of PAFc (Wu and Xu 2012). ChIP-seq (ChIP combined with deep sequencing) analyses of all of the PAFc subunits will help clarify the dependence or independence of PAFc subunits in the context of the ERα regulatory network. As shown in a recent study (Chen et al. 2015), a high-quality ChIP-grade antibody for Ctr9 is not yet available.

Materials and methods

Cell culture and reagents

HEK293T, MCF-7, T47D, and MDA-MB-231 cells were obtained from American Type Culture Collection (ATCC) and maintained in Dulbecco's modified medium (DMEM) (Life Technologies) supplemented with 10% fetal bovine serum (FBS) (Life Technologies). BT474 cells were obtained from ATCC and maintained in RPMI 1640 medium supplemented with 10% FBS. Estrogen-independent LCC1 cells and tamoxifen-resistant LCC2 cells were a gift from Dr. Robert Clarke (Georgetown University) and maintained in DMEM supplemented with 10% FBS. MCF7-tet-on parental cells and MCF7-tet-on–shCtr9 cells were generated previously and maintained in DMEM supplemented with 10% FBS. All cells were cultured at 37°C in a humidified atmosphere containing 5% CO_2. Dox was purchased from Clontech and used at a final concentration of 500 ng/mL. DMSO, E2, 4-OHT, CHX, and MG132 were purchased from Sigma. E2 induction experiments were carried out by changing the cell culture medium to phenol red-free DMEM supplemented with 5% charcoal–dextran-treated FBS (stripped medium) 3 d prior to E2 treatment.

Cell proliferation and two-dimensional (2D) colony formation assays

For cell counting-based proliferation assays, 1×10^5 cells were seeded in triplicate into six-well plates. For the MCF7-tet-on–shCtr9 cell line, cells were pretreated with vehicle or 500 ng/mL Dox for 4 d and then seeded into six-well plates. Media were refreshed every 48 h. Cells were trypsinized and counted after Trypan blue exclusion using an automated cell counter (Bio-Rad) according to the manufacturer's protocol. For 3-(4,5-dimethylthiazol-2-yl)-2,5-diphenyltetrazolium (MTT)-based (Sigma-Aldrich) proliferation assays, 2×10^3 cells were seeded into 96-well plates and treated with corresponding compounds. Fifteen microliters of MTT (5 mg/mL in DPBS) was added to the cells followed by incubation for 1 h at 37°C. After removing the cell culture medium, 50 µL of DMSO was added, the absorbance of the color substrate was measured with a 540-nm filter on a Victor X5 microplate reader (Perkin Elmer), and data were plotted and analyzed by GraphPad Prism 5 software (GraphPad Software, Inc.). For 2D colony formation assays, 100 cells were seeded into six-well plates (or 1000 cells were seeded into a 10-cm dish) and treated with corresponding compounds. Media were refreshed every 4 d. After 2 wk, cells were washed with DPBS, fixed with 4% formaldehyde for 10 min at room temperature, stained with 0.05% crystal violet for 30 min at room temperature, and then imaged on a Leica inverted microscope using the Leica Application Suite software. Colony numbers were counted using ImageJ software.

Flow cytometry analyses and senescence-associated β-galactosidase staining

To assess the cell cycle distribution, MCF7-tet-on–shCtr9 cells were cultured as described above and treated with vehicle or 500 ng/mL Dox for 7 d. Cells were collected by trypsinization, fixed in cold 95% ethanol, and washed in PBS. The fixed cells were then resuspended in propidium iodide staining solution (200 µg/mL RNase A, 50 µg/mL propidium iodide, 0.1% [v/v] Triton X-100 in PBS + 1% BSA) and incubated overnight at 4°C. Samples were analyzed by flow cytometry at the University of Wisconsin Flow Cytometry Laboratory. Data were analyzed using FlowJo software (Tree Star). For senescence-associated β-galactosidase staining, cells were fixed in a 2% formaldehyde/0.2% glutaraldehyde solution for 5 min and then stained overnight at 37°C with an X-Gal-containing staining buffer. After two PBS washes, cells

were imaged on a Leica inverted microscope using the Leica Application Suite software.

Gene expression analyses by human transcriptome array 2.0

To globally identify Ctr9-regulated genes, MCF7-tet-on–shCtr9 cells were cultured in DMEM supplemented with 10% FBS in the absence or presence of 500 ng/mL Dox for 4 d followed by continuing culture in stripped medium in the absence or presence of 500 ng/mL Dox for another 3 d. Cells were then treated with DMSO or 10 nM E2 for 4 h prior to cell collection. Total RNA was extracted using a Qiagen RNeasy Plus kit according to the manufacturer's protocol, and three independent experiments were performed. Purified total RNA was submitted to the University of Wisconsin Madison Biotechnology Center for RNA quality analysis, reverse transcription, labeling, and hybridization to the Affymetrix human transcriptome array 2.0 containing >6.0 million distinct probes covering 44,699 protein-coding genes and 22,829 non-protein-coding genes. Data analysis and visualization were performed using the Affymetrix Transcriptome Analysis Console (TAC) software. The criteria for selecting differentially expressed genes was a 1.5-fold change cutoff and a FDR of <0.05. Data are available at Gene Expression Omnibus (GEO) under accession number GSE73388. Pathway enrichments and functional analyses of the gene lists were determined using ingenuity pathway analysis (IPA) software (Ingenuity Systems).

Human breast cancer TMA immunohistochemistry (IHC)

Human breast cancer TMAs constructed by the University of Wisconsin Carbone Cancer Center included tumors from 372 individual subjects with stage I to stage III breast cancer treated from 1999 to 2007. Tumor blocks were identified from eligible cases and reviewed by a certified pathologist for adequacy. Tumor sites were marked, and then triplicate 0.6-mm punch biopsies were obtained. Samples were linked to a coded database with clinical data that was obtained from the University of Wisconsin Hospital and Clinics Cancer Registry and manual chart review. All cases had at least 5 years of follow-up or recurrence or death within the 5 yr. The University of Wisconsin Health Sciences Institutional Review Board (IRB) approved the TMA creation and waived IRB approval for future use of the TMA and coded data set. For Ctr9 IHC, TMA slides were deparaffinized and rehydrated in xylenes and ethanol followed by heat-induced antigen retrieval in 10 mM citrate buffer (pH 6.0). TMA slides were then blocked by Peroxidazed I, Background Punisher, Avidin, and Biotin consecutively, following the manufacturer's protocol (Biocare Medical). Tissue sections were then incubated with Ctr9 antibody (1:200; ab84487) overnight at 4°C. After washing with TBST (50 mM Tris-HCl, 150 mM NaCl, 0.05% Tween-20 at pH 7.4), biotinylated goat anti-rabbit IgG (Biocare Medical) was applied to TMA slides with incubation for 15 min at room temperature. After TBST wash, TMA slides were incubated with Streptavidin-HRP (Biocare Medical) for 15 min at room temperature and then rinsed with TBST. Subsequently, TMA slides were incubated with diluted DAB Chromogen (Biocare Medical) and counterstained with Biocare Medical CAT hematoxylin solution. After washing, the TMA slides were dehydrated in xylenes and ethanol and air-dried prior to mounting using Cytoseal mounting medium in the fume hood. The stained TMA slides were then image-scanned and analyzed.

Quantitation of Ctr9 IHC staining intensity

Vectra (PerkinElmer) was used for quantitation of the Ctr9 IHC staining on TMA slides. This system includes an automated slide scanner and image processing software Nuance and inForm. The Ctr9 staining intensity was quantitated in two steps, including image acquisition and data analysis. For image acquisition, two control breast tissue slides stained with one dye only (DAB dye and hematoxylin, respectively) were used to build a spectral library for nonmixed signals (DAB and hematoxylin) for the following quantitation. The Ctr9 IHC TMA slides were loaded onto the Vectra slide scanner. A scanning protocol, including a spectral library, was created based on the TMA size, areas of interest, and staining complexity (single or multiple staining in a single section). Eight-bit image cubes were acquired for further analysis. For data analysis, inForm software was used for tissue (breast epithelium vs. stroma) and cell (nucleus vs. cytoplasm) segmentations. The spectral library was used to unmix the signals on the image cubes with dual colors (DAB and hematoxylin) by recognizing their unique spectral curves, eliminating the signal noises and cross-talk. Ctr9 IHC intensity was then quantitated with the nuclear compartment, and mean optical density data were collected. Fifty samples were first trained to configure and fine-tune the image preparation, segmentation, and scoring. The fine-tuned settings were exported and applied to the whole set of samples on the TMA slides for quantitation of Ctr9 IHC intensity (mean optical density). Statistical analyses were performed to examine the relationship between the Ctr9 level (mean optical density) and the clinical outcomes. The samples were divided into low Ctr9 and high Ctr9 groups based on the median value of the mean optical density. The survival curves were generated using the Kaplan-Meier method. The distribution of the survival functions for the Ctr9 level groups were tested using the log-rank test. Figures were generated using GraphPad Prism 5 software (Graph-Pad Software, Inc.).

Additional information on antibodies, shRNAs, and primers is available in the Supplemental Material.

Acknowledgments

We thank Dr. Alana L Welm for kindly providing the patient-derived tumor graft samples, Dr. Robert Clarke for providing MCF7/LCC1 and MCF7/LCC2 cell lines and the corresponding parental MCF7 cells, Dr. Sandeep Saha and Dr. Menggang Yu for assistance in some preliminary data analysis, and Dr. Wei Huang for scanning the optical density of IHC staining. This project was supported by Department of Defense ERA of Hope Award W81XWYH-11-1-0237 to W.X. H.Z. and W.X. conceived and designed the experiments. H.Z. performed the experiments and data analyses. H.Z. wrote the manuscript, and W.X. edited the manuscript.

References

Al-Dhaheri M, Wu J, Skliris GP, Li J, Higashimato K, Wang Y, White KP, Lambert P, Zhu Y, Murphy L, et al. 2011. CARM1 is an important determinant of ERα-dependent breast cancer cell differentiation and proliferation in breast cancer cells. *Cancer Res* **71:** 2118–2128.

Barone I, Brusco L, Gu G, Selever J, Beyer A, Covington KR, Tsimelzon A, Wang T, Hilsenbeck SG, Chamness GC, et al. 2011. Loss of Rho GDIα and resistance to tamoxifen via effects on estrogen receptor α. *J Natl Cancer Inst* **103:** 538–552.

Bashyam MD, Bair R, Kim YH, Wang P, Hernandez-Boussard T, Karikari CA, Tibshirani R, Maitra A, Pollack JR. 2005. Array-based comparative genomic hybridization identifies localized DNA amplifications and homozygous deletions in pancreatic cancer. *Neoplasia* **7:** 556–562.

Betz JL, Chang M, Washburn TM, Porter SE, Mueller CL, Jaehning JA. 2002. Phenotypic analysis of Paf1/RNA polymerase II

complex mutations reveals connections to cell cycle regulation, protein synthesis, and lipid and nucleic acid metabolism. *Mol Genet Genomics* **268:** 272–285.

Bostner J, Skoog L, Fornander T, Nordenskjöld B, Stål O. 2010. Estrogen receptor-α phosphorylation at serine 305, nuclear p21-activated kinase 1 expression, and response to tamoxifen in postmenopausal breast cancer. *Clin Cancer Res* **16:** 1624–1633.

Camps J, Armengol G, del Rey J, Lozano JJ, Vauhkonen H, Prat E, Egozcue J, Sumoy L, Knuutila S, Miró R. 2006. Genome-wide differences between microsatellite stable and unstable colorectal tumors. *Carcinogenesis* **27:** 419–428.

Carpten JD, Robbins CM, Villablanca A, Forsberg L, Presciuttini S, Bailey-Wilson J, Simonds WF, Gillanders EM, Kennedy AM, Chen JD, et al. 2002. HRPT2, encoding parafibromin, is mutated in hyperparathyroidism-jaw tumor syndrome. *Nat Genet* **32:** 676–680.

Chaudhary K, Deb S, Moniaux N, Ponnusamy MP, Batra SK. 2007. Human RNA polymerase II-associated factor complex: dysregulation in cancer. *Oncogene* **26:** 7499–7507.

Chen D, Ma H, Hong H, Koh SS, Huang SM, Schurter BT, Aswad DW, Stallcup MR. 1999. Regulation of transcription by a protein methyltransferase. *Science* **284:** 2174–2177.

Chen FX, Woodfin AR, Gardini A, Rickels RA, Marshall SA, Smith ER, Shiekhattar R, Shilatifard A. 2015. PAF1, a molecular regulator of promoter-proximal pausing by RNA polymerase II. *Cell* **162:** 1003–1015.

Chu X, Qin X, Xu H, Li L, Wang Z, Li F, Xie X, Zhou H, Shen Y, Long J. 2013. Structural insights into Paf1 complex assembly and histone binding. *Nucleic Acids Res* **41:** 10619–10629.

Cleator SJ, Ahamed E, Coombes RC, Palmieri C. 2009. A 2009 update on the treatment of patients with hormone receptor-positive breast cancer. *Clin Breast Cancer* **9:** S6–S17.

Crisucci EM, Arndt KM. 2011. The roles of the Paf1 complex and associated histone modifications in regulating gene expression. *Genet Res Int* doi: 10.4061/2011/707641.

Deroo BJ, Korach KS. 2006. Estrogen receptors and human disease. *J Clin Invest* **116:** 561–570.

Droog M, Beelen K, Linn S, Zwart W. 2013. Tamoxifen resistance: from bench to bedside. *Eur J Pharmacol* **717:** 47–57.

Giamas G, Filipović A, Jacob J, Messier W, Zhang H, Yang D, Zhang W, Shifa BA, Photiou A, Tralau-Stewart C, et al. 2011. Kinome screening for regulators of the estrogen receptor identifies LMTK3 as a new therapeutic target in breast cancer. *Nat Med* **17:** 715–719.

Hanks S, Perdeaux ER, Seal S, Ruark E, Mahamdallie SS, Murray A, Ramsay E, Del Vecchio Duarte S, Zachariou A, de Souza B, et al. 2014. Germline mutations in the PAF1 complex gene CTR9 predispose to Wilms tumour. *Nat Commun* **5:** 4398.

Hattrup CL, Gendler SJ. 2006. MUC1 alters oncogenic events and transcription in human breast cancer cells. *Breast Cancer Res* **8:** R37.

Jaehning JA. 2010. The Paf1 complex: platform or player in RNA polymerase II transcription? *Biochim Biophys Acta* **1799:** 379–388.

Jézéquel P, Frénel JS, Campion L, Guérin-Charbonnel C, Gouraud W, Ricolleau G, Campone M. 2013. bc-GenExMiner 3.0: new mining module computes breast cancer gene expression correlation analyses. *Database (Oxford)* **2013:** bas060.

Jiang P, Enomoto A, Takahashi M. 2009. Cell biology of the movement of breast cancer cells: intracellular signalling and the actin cytoskeleton. *Cancer Lett* **284:** 122–130.

Jørgensen L, Brünner N, Spang-Thomsen M, James MR, Clarke R, Dombernowsky P, Svenstrup B. 1997. Steroid metabolism in the hormone dependent MCF-7 human breast carcinoma cell line and its two hormone resistant subpopulations MCF-7/LCC1 and MCF-7/LCC2. *J Steroid Biochem Mol Biol* **63:** 275–281.

Kharbanda A, Rajabi H, Jin C, Raina D, Kufe D. 2013. Oncogenic MUC1-C promotes tamoxifen resistance in human breast cancer. *Mol Cancer Res* **11:** 714–723.

Kim J, Guermah M, Roeder RG. 2010. The human PAF1 complex acts in chromatin transcription elongation both independently and cooperatively with SII/TFIIS. *Cell* **140:** 491–503.

Kininis M, Isaacs GD, Core LJ, Hah N, Kraus WL. 2009. Postrecruitment regulation of RNA polymerase II directs rapid signaling responses at the promoters of estrogen target genes. *Mol Cell Biol* **29:** 1123–1133.

Koch C, Wollmann P, Dahl M, Lottspeich F. 1999. A role for Ctr9p and Paf1p in the regulation G1 cyclin expression in yeast. *Nucleic Acids Res* **27:** 2126–2134.

Le Romancer M, Treilleux I, Leconte N, Robin-Lespinasse Y, Sentis S, Bouchekioua-Bouzaghou K, Goddard S, Gobert-Gosse S, Corbo L. 2008. Regulation of estrogen rapid signaling through arginine methylation by PRMT1. *Mol Cell* **31:** 212–221.

Levin ER. 2005. Integration of the extranuclear and nuclear actions of estrogen. *Mol Endocrinol* **19:** 1951–1959.

Lin L, Zhang JH, Panicker LM, Simonds WF. 2008. The parafibromin tumor suppressor protein inhibits cell proliferation by repression of the c-myc proto-oncogene. *Proc Natl Acad Sci* **105:** 17420–17425.

Madak-Erdogan Z, Ventrella R, Petry L, Katzenellenbogen BS. 2014. Novel roles for ERK5 and cofilin as critical mediators linking ERα-driven transcription, actin reorganization, and invasiveness in breast cancer. *Mol Cancer Res* **12:** 714–727.

Massoni-Laporte A, Perrot M, Ponger L, Boucherie H, Guieysse-Peugeot AL. 2012. Proteome analysis of a CTR9 deficient yeast strain suggests that Ctr9 has function(s) independent of the Paf1 complex. *Biochim Biophys Acta* **1824:** 759–768.

Mohammed H, D'Santos C, Serandour AA, Ali HR, Brown GD, Atkins A, Rueda OM, Holmes KA, Theodorou V, Robinson JL, et al. 2013. Endogenous purification reveals GREB1 as a key estrogen receptor regulatory factor. *Cell Rep* **3:** 342–349.

Moniaux N, Nemos C, Schmied BM, Chauhan SC, Deb S, Morikane K, Choudhury A, Vanlith M, Sutherlin M, Sikela JM, et al. 2006. The human homologue of the RNA polymerase II-associated factor 1 (hPaf1), localized on the 19q13 amplicon, is associated with tumorigenesis. *Oncogene* **25:** 3247–3257.

Mueller CL, Porter SE, Hoffman MG, Jaehning JA. 2004. The Paf1 complex has functions independent of actively transcribing RNA polymerase II. *Mol Cell* **14:** 447–456.

Neve RM, Chin K, Fridlyand J, Yeh J, Baehner FL, Fevr T, Clark L, Bayani N, Coppe JP, Tong F, et al. 2006. A collection of breast cancer cell lines for the study of functionally distinct cancer subtypes. *Cancer Cell* **10:** 515–527.

Pawitan Y, Bjöhle J, Amler L, Borg AL, Egyhazi S, Hall P, Han X, Holmberg L, Huang F, Klaar S, et al. 2005. Gene expression profiling spares early breast cancer patients from adjuvant therapy: derived and validated in two population-based cohorts. *Breast Cancer Res* **7:** R953–R964.

Perou CM, Sørlie T, Eisen MB, van de Rijn M, Jeffrey SS, Rees CA, Pollack JR, Ross DT, Johnsen H, Akslen LA, et al. 2000. Molecular portraits of human breast tumours. *Nature* **406:** 747–752.

Peterlin BM, Price DH. 2006. Controlling the elongation phase of transcription with P-TEFb. *Mol Cell* **23:** 297–305.

Pirngruber J, Shchebet A, Schreiber L, Shema E, Minsky N, Chapman RD, Eick D, Aylon Y, Oren M, Johnsen SA. 2009. CDK9 directs H2B monoubiquitination and controls replication-

dependent histone mRNA 3′-end processing. *EMBO Rep* **10:** 894–900.

Pitroda SP, Khodarev NN, Beckett MA, Kufe DW, Weichselbaum RR. 2009. MUC1-induced alterations in a lipid metabolic gene network predict response of human breast cancers to tamoxifen treatment. *Proc Natl Acad Sci* **106:** 5837–5841.

Prenzel T, Begus-Nahrmann Y, Kramer F, Hennion M, Hsu C, Gorsler T, Hintermair C, Eick D, Kremmer E, Simons M, et al. 2011. Estrogen-dependent gene transcription in human breast cancer cells relies upon proteasome-dependent monoubiquitination of histone H2B. *Cancer Res* **71:** 5739–5753.

Rayala SK, Molli PR, Kumar R. 2006a. Nuclear p21-activated kinase 1 in breast cancer packs off tamoxifen sensitivity. *Cancer Res* **66:** 5985–5988.

Rayala SK, Talukder AH, Balasenthil S, Tharakan R, Barnes CJ, Wang RA, Aldaz CM, Khan S, Kumar R. 2006b. P21-activated kinase 1 regulation of estrogen receptor-α activation involves serine 305 activation linked with serine 118 phosphorylation. *Cancer Res* **66:** 1694–1701.

Rozenblatt-Rosen O, Hughes CM, Nannepaga SJ, Shanmugam KS, Copeland TD, Guszczynski T, Resau JH, Meyerson M. 2005. The parafibromin tumor suppressor protein is part of a human Paf1 complex. *Mol Cell Biol* **25:** 612–620.

Tarkkanen M, Larramendy ML, Böhling T, Serra M, Hattinger CM, Kivioja A, Elomaa I, Picci P, Knuutila S. 2006. Malignant fibrous histiocytoma of bone: analysis of genomic imbalances by comparative genomic hybridisation and C-MYC expression by immunohistochemistry. *Eur J Cancer* **42:** 1172–1180.

Tomson BN, Arndt KM. 2013. The many roles of the conserved eukaryotic Paf1 complex in regulating transcription, histone modifications, and disease states. *Biochim Biophys Acta* **1829:** 116–126.

Vaz AP, Ponnusamy MP, Rachagani S, Dey P, Ganti AK, Batra SK. 2014. Novel role of pancreatic differentiation 2 in facilitating self-renewal and drug resistance of pancreatic cancer stem cells. *Br J Cancer* **111:** 486–496.

Wei X, Xu H, Kufe D. 2006. MUC1 oncoprotein stabilizes and activates estrogen receptor α. *Mol Cell* **21:** 295–305.

Wittmann BM, Fujinaga K, Deng H, Ogba N, Montano MM. 2005. The breast cell growth inhibitor, estrogen down regulated gene 1, modulates a novel functional interaction between estrogen receptor α and transcriptional elongation factor cyclin T1. *Oncogene* **24:** 5576–5588.

Wu J, Xu W. 2012. Histone H3R17me2a mark recruits human RNA polymerase-associated factor 1 complex to activate transcription. *Proc Natl Acad Sci* **109:** 5675–5680.

Youn MY, Yoo HS, Kim MJ, Hwang SY, Choi Y, Desiderio SV, Yoo JY. 2007. hCTR9, a component of Paf1 complex, participates in the transcription of interleukin 6-responsive genes through regulation of STAT3–DNA interactions. *J Biol Chem* **282:** 34727–34734.